Targeted molecular dynamics simulation studies of binding and conformational changes in E. coli MurD

ARTICLE *in* PROTEINS STRUCTURE FUNCTION AND BIOINFORMATICS · JULY 2007

Impact Factor: 2.63 · DOI: 10.1002/prot.21374 · Source: PubMed

4 AUTHORS, INCLUDING:

Andrej Perdih
National Institute of Chemistry
44 PUBLICATIONS **439** CITATIONS

SEE PROFILE

Miha Kotnik
Sandoz
15 PUBLICATIONS **397** CITATIONS

SEE PROFILE

Tom Solmajer
National Institute of Chemistry
98 PUBLICATIONS **1,241** CITATIONS

SEE PROFILE

PROTEINS: Structure, Function, and Bioinformatics 68:243–254 (2007)

Targeted Molecular Dynamics Simulation Studies of Binding and Conformational Changes in *E. coli* MurD

Andrej Perdih,[1] Miha Kotnik,[2] Milan Hodoscek,[1] and Tom Solmajer[1,2]*
[1]*Laboratory for Molecular Modelling and NMR Spectroscopy, National Institute of Chemistry, Hajdrihova 19, 1001 Ljubljana, Slovenia*
[2]*Lek Pharmaceuticals d.d., Drug Discovery, Verovškova 57, 1526 Ljubljana, Slovenia*

ABSTRACT **Enzymes involved in the biosynthesis of bacterial peptidoglycan, an essential cell wall polymer unique to prokaryotic cells, represent a highly interesting target for antibacterial drug design. Structural studies of *E. coli* MurD, a three-domain ATP hydrolysis driven muramyl ligase revealed two inactive open conformations of the enzyme with a distinct C-terminal domain position. It was hypothesized that the rigid body rotation of this domain brings the enzyme to its closed active conformation, a structure, which was also determined experimentally. Targeted molecular dynamics 1 ns-length simulations were performed in order to examine the substrate binding process and gain insight into structural changes in the enzyme that occur during the conformational transitions into the active conformation. The key interactions essential for the conformational transitions and substrate binding were identified. The results of such studies provide an important step toward more powerful exploitation of experimental protein structures in structure-based inhibitor design. Proteins 2007;68:243–254.** © 2007 Wiley-Liss, Inc.

Key words: targeted molecular dynamics (TMD); MurD; domain movements; binding process; molecular simulation

INTRODUCTION

Bacterial resistance to antibiotics has underlined an urgent need for the discovery of novel efficacious antibacterial agents directed towards previously unexploited targets.[1,2] As an essential bacterial cell-wall polymer unique to prokaryotic cells, peptidoglycan represents an optimal target with respect to selective toxicity. Properly constructed peptidoglycan provides the rigidity, flexibility, and strength that are necessary for bacterial cells to grow and divide while withstanding high internal osmotic pressure.[3]

The biosynthesis of peptidoglycan is a complex multistage process involving early stage intracellular assembly of the UDP-MurNAc pentapeptide, which is subsequently translocated to the extracellular side, where it is ultimately incorporated into the nascent biopolymer. Four UDP-*N*-acetyl muramyl ligases, MurC, MurD, MurE, and MurF catalyze intracellular assembly of the peptide moiety by consecutive addition of L-Ala, D-Glu, *meso*-DAP (or L-Lys) and D-Ala-D-Ala to the starting UDP-precursor (UDP-MurNAc).[4]

All four members of the Mur ligase family share a close structural and functional resemblance. Comparison of the published crystal structures revealed that they all share the same three-domain topology with the N-terminal and central domain primarily responsible for binding of the UDP-precursor and ATP molecule, which activates amide bond synthesis.[5–7] The condensing amino acid residue subsequently binds to the C-terminal part of the ligase. Initial velocity and dead-end inhibitor studies on MurC and fused form of MurF were consistent with an ordered kinetic mechanism in which ATP binds first to the free enzyme, followed by a corresponding UDP-precursor and the amino acid binding last.[8,9] Despite the surprising fact that sequence alignment of Mur ligase orthologs and paralogs showed relatively low overall homology alignment comparison of the residues comprising the active sites reached quite high homology scores. The ATP binding pocket in particular seems to be well conserved throughout the family.[10,11]

MurD (UDP-*N*-acetylmuramoyl-L-alanine:D-glutamate ligase), the second enzyme in the ligase series, catalyses the highly specific incorporation of D-glutamate into the cytoplasmic intermediate UDP-*N*-acetyl-muramoyl-L-alanine (UMA). Several structures of *E.coli* MurD (PDB entries: 1UAG-4UAG), which revealed the enzyme active conformation accompanied by the positions and binding pattern of UMA, ADP (hydrolyzed form of ATP) (PDB: 2UAG and 3UAG) and the conformation of the product of the enzyme reaction UMAG (PDB: 4UAG) were determined by Dideberg and coworkers.[5,6] Frequently referred to as "closed" structures, these conformations of MurD comprise three domains of topology each reminiscent of nucleotide-binding folds: the N- and C-terminal domains are consistent with the dinucleotide-binding Rossmann

Grant sponsor: European Union (FP6 Integrated Project EURINTAFAR); Grant number: LSHM-CT-2004-512138; Grant sponsor: Ministry of Higher Education, Science and Technology, Republic of Slovenia.

*Correspondence to: Tom Solmajer, National Institute of Chemistry, Hajdrihova 19, 1001 Ljubljana, Slovenia. E-mail: tom.solmajer@ki.si

Received 28 July 2006; Revised 20 November 2006; Accepted 12 December 2006

Published online 11 April 2007 in Wiley InterScience (www.interscience.wiley.com). DOI: 10.1002/prot.21374

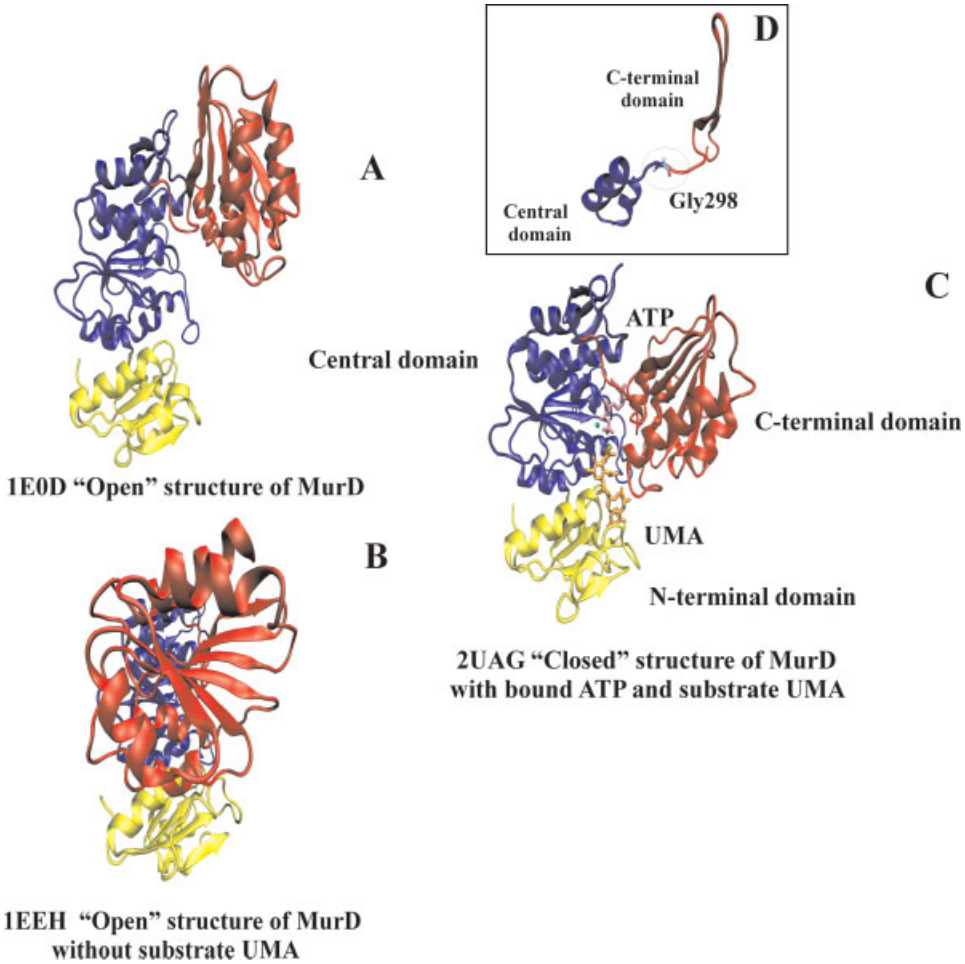

Fig. 1. Protein structures used in the TMD simulation. The central and N-terminal domain of all respective MurD structures (relaxed 1E0D, 1EEH, and 2UAG) were superimposed and each structure is presented separately for clarity. (**A**) Relaxed open structure of MurD based on the crystal structure 1E0D of Dideberg and coworkers.[7] The N-terminal domain is denoted in yellow, the central domain in blue and the C-terminal domain is depicted in red. (**B**) Relaxed open structure of MurD based on the crystal structure 1EEH of Dideberg and coworkers[7] (same color scheme). (**C**) Relaxed closed structure of MurD based on the crystal structure 2UAG of Dideberg and coworkers (same color scheme).[6] The C-terminal domain in this conformation is positioned to form the active conformation of the enzyme. (**D**) Gly298 positioned at the end of the central domain is located near the proposed hinge axis origin of the rigid body rotation.

fold, and the central domain with the mononucleotide-binding fold also observed in the GTPase family [Fig. 1(C)]. Structural studies also identified two magnesium-binding sites that bridge negatively charged groups of UMA and ATP. The first, located between the ADP and UMA moieties, was proposed to assist in phosphoryl transfer between the two anionic substrates while the other, presumably positioned between the β- and γ-phosphate groups of ATP, is believed to play a vital role in the phosphate transfer to yield the acyl-phosphate intermediate

Further X-ray experiments revealed two MurD structures, termed "open" structures, where the C-terminal domain undergoes a large rigid-body rotation away from the N-terminal and central domain. These structures, crystallized in the presence (PDB entry: 1EEH) and absence (PDB entry: 1E0D) of substrate UMA, resulted in two entirely different C-terminal domain positions. Using a hinge axis origin located near Gly298 at the end of the central domain [Fig. 1(D)], a 50° rigid-body rotation was hypothesized as being required to bring the first "open" structure (1E0D) to its "closed" form.[7] The novel position of the C-terminal domain remained in the same plane as the central and N-terminal domain, similar to closed structures of MurD [Fig. 1(A)]. Surprisingly, the position of the C-terminal domain in open MurD *co*-crystallized with UMA (1EEH) was found to be significantly different indicating a 109° rigid-body rotation around the same hinge axis that, in contrast to other open structure, occurs out of the original plane so that the C-terminal domain rests on the top of the N-and central domains. [Fig. 1(B)].[7] It was suggested that binding of ATP to MurD is required for closure of the enzyme as crystallographic studies indicated that the UDP sub-

strate (UMA) alone is unable to induce the domain closure.[7] Rotation of the C-terminal domain has also been observed for the MurF enzyme, where recent structural studies of the *Streptococcus pneumoniae* species revealed, that the inhibitor binding can induce the domain closure, even yielding a "closed" conformation of the ligase dissimilar to the expected transition state conformation for this enzyme family.[12,13]

Current knowledge about the enzymes of the Mur ligase family indicates that the C-terminal domain undergoes a large conformational change after ATP binds to the enzyme thereby, forming the closed "active" conformation of the enzyme, that enables amide bond formation to take place. In principle various pathways of conformational change, leading to the active form of the enzyme, are possible. A description of conformational changes accompanied by details about UMA and ATP binding at the atomic level would provide additional details of the MurD mechanism not attainable with the experiment. Moreover, the information obtained could be of value in the design of new MurD inhibitors for which detailed knowledge of the binding pockets is requested.

Molecular dynamics (MD) simulations of biomolecules constitute an important tool for understanding the physical basis of the structure and function of biological macromolecules. In atomistic MD simulations, the atomic vibrations limit the maximum time step to a few femtoseconds (fs) to maintain the integration stability. Molecular processes involving large conformational changes, such as domain movements, for example, takes place at the microsecond to millisecond time scale and are presently beyond the reach of atomistic MD simulations.[14–16] To enable simulations of such large conformational transitions biasing techniques have been developed that drive the trajectory from the initial to the final state, with both being known from high-resolution structural studies. It is obvious that none of the available methods is fully satisfactory. One extensively exploited method is Targeted Molecular Dynamics (TMD) developed by Schlitter et al.,[17,18] who generates the trajectory of the conformational transition by using an additional force that decreases the RSMD (Root mean square distance) between the starting and target molecular conformation.[19–21]

In the present study, we report two dynamic models of the C-terminal domain closing motion in MurD ligase accompanied by a description of the UDP precursor (UMA) and ATP binding as determined with the TMD simulation. Although the TMD method was primarily designed to study conformational changes we were also interested to examine if this method could also provide insight into the substrate binding process, since the biochemical data regarding the binding order are available for this enzyme family.[8,9]

METHODS

All calculations were carried out on CROW clusters at the National Institute of Chemistry, Ljubljana, Slovenia[22] utilizing CHARMM molecular modeling suite.[23] Experimentally solved open and closed structures of the MurD enzyme, which represented the starting coordinates for molecular simulation, were retrieved from the Protein Data Bank: PDB entries 2UAG, (closed structure)[6] and 1EEH, 1E0D (open structures).[7] Hydrogen atoms were added to the amino acid residues using the HBUILD routine. In each of the investigated MurD conformations, some amino acid residues were not visible in the experimental electron density map. In the case of 2UAG these amino acids comprised the sequences of residues 221–224 and 242–244 respectively; 1EEH lacks residues 240–245 and in 1E0D the residues between 183–188 and 221–224 are not provided. Missing residues were constructed using CHARMM and the system was subjected to energy minimization using the modified Adopted Basis Newton-Raphson method in 200 steps and was further relaxed in the implicit solvent (GBSW model) for 100 ps. The excessive electron density, which was found on Nζ of Lys198 in the crystal structure, was previously interpreted to be a carboxylic group, yielding the carbamate derivative of the Lys198 amino group (KCX residue).[6] Furthermore, it was suggested on the basis of chemical rescue experiments that this residue plays an important role in the formation of magnesium binding site in Mur ligases.[24] This structural modification of Lys224 was also observed in *E. coli* MurE where carbamylated Lys224 is present in the active site and presumably plays the same role as modified Lys198.[25] Interestingly, both experimental open structures lacked the modification of Lys198 observed in closed structures of MurD. The absence of this modification in the open structures was attributed to the crystallization conditions of the protein at pH 6.[7] CHARMM parameter and topology files (version 27) for proteins[26,27] and nucleic acids[28,29] were utilized to specify force field parameters describing the protein, substrate UMA, ATP, and carbamylated Lys198 residue.

The third phosphate group was added to ADP to conduct the simulations with a fully functional ATP. The phosphate group was positioned as suggested by Dideberg and coworkers, by positioning one oxygen as a ligand for the Mg^{2+} located in the pocket between UMA and ADP and the other coordinated with Nζ of Lys115.[6] In both open structures (1EEH, 1E0D) of MurD, the Lys198 was changed to its carbamylated form as observed in the closed structure. Both Mg^{2+} ions and the ATP molecule were included in 1EEH and 1E0D to complete the enzyme composition. Subsequently, Mg^{2+} ions, ATP, and UMA were positioned in the nearby surroundings of the open structures in order to provide a satisfactory description of the system prior to substrate binding. The final system prepared for the TMD simulation comprised 6692 atoms in all structures. Two pathways of conformational change were calculated using 2UAG and 1EEH (1EEH-2UAG trajectory) and 2UAG and 1E0D (1E0D-2UAG trajectory), respectively, as boundary closed and open conformations of MurD.

To test the suitability of the implicit solvent model that was employed in TMD simulations 1EEH structure

was immersed into a cubic box (100 Å × 100 Å × 100 Å) of water molecules.[30] Deletion of the waters overlapping with the protein resulted in a system with ~30,000 TIP3 waters. Electrostatic interactions were computed with the particle-mesh-Ewald method.[31] After initial water relaxation for 50 ps whole system was relaxed for an additional 50 ps. This simulation was used for the comparison with the simulation performed in an implicit solvent environment using the generalized Born model with simple smoothing functions (GBSW model)[32] as implemented in CHARMM. Atomic Born radii for the amino acids were parameterized according to Nina et al.[33] MD simulations of 100 ps were conducted for both structures and the results were analyzed and compared with those obtained from the explicit water simulation.

Observed RMSD differences for all atoms (0.8 Å) and main chain atoms (0.7 Å) respectively for the crystalographically determined structure 1EEH are within expected limits compared with results from explicit waters environment (0.7 Å and 0.4 Å for all atoms and main-chain atoms). Additionally, in the 2UAG structure the hydrogen-bonding networks between the ligands and the residues of the respective binding pockets, as well as coordination of both Mg^{2+} ions, remained intact displaying the preserved main features of the crystal structure. The results indicate sufficient appropriateness of the implicit GBSW model for further exploitation in the time-demanding TMD simulations.

Visualization of all treated systems throughout this study was done via VMD software[34] where the STRIDE program was utilized for the secondary structure generation.[35] Graphical interpretation of the results was performed via the Gnuplot program.[36]

The CHARMM all-atom potential energy function was used to calculate the TMD trajectories. TMD as implemented in CHARMM employs a standard molecular mechanics potential and adds a time-dependent holonomic constraint [Eq. (1)] to reduce the root mean square deviation (RMSD) from a known initial structure to a known target structure by each MD step.[17,18]

$$\Phi[X(t)] = \sum [X_{\mathrm{i}}(t) - X_{T_{\mathrm{i}}}]^2 - \rho(t) = 0 \qquad (1)$$

$X_{\mathrm{i}}(t)$ in Eq. (1) represents the position of the atom i at time t, X_{Ti} is the target position, $\rho(t)$ is the desired RMSD, and the sum is over all atoms. The underlines indicate that the coordinates are scaled by $\sqrt{m_{\mathrm{i}}/\langle m_{\mathrm{i}}\rangle}$; where m_{i} is the mass of atom i and $\langle m_{\mathrm{i}}\rangle$ is the average atom mass. This mass scaling removes the net translation of the system.[37] The additional constraining force is expressed as [Eq. (2)]:

$$F_{\mathrm{i}}^{C} = \lambda \times \nabla\phi = \frac{2\lambda \times m_{\mathrm{i}}}{\langle m_{\mathrm{i}}\rangle}(X_{\mathrm{i}} - X_{T_{\mathrm{i}}}) \qquad (2)$$

where λ is an adjustable Lagrange parameter. The initial RMSD differences of 17.3 Å (between 2UAG and 1EEH) and 9.22 Å (between 2UAG and 1E0D) were reduced gradually by the TMD increments of 0.000016 Å and 0.000008 Å to account for approximately the same simulation time. The constraining force was applied to all atoms. A time step of 1 fs was used for the dynamics with a leapfrog integration scheme[38] and the temperature was held constant at 300 K. Coordinates were saved every 100 fs. The resulting TMD trajectories were completed in ~1 ns.

The TMD trajectories describing binding and conformational change were calculated in reverse direction stating from closed conformation (2UAG) proceeding to the final open state (1EEH or 1E0D). The main reason for this direction reversal is that the closed state of MurD represents an experimentally determined configuration of system also in terms of ligand positions. As the TMD procedure normally finds a successive configuration, which can be reached from the previous one with a minimum energy expenditure,[17,18] this course of simulation most probably provides a better starting representation for the simulation than the open structure with arbitrary ligands positions. However, the description of binding events and rotational motion will be described in the direction from open to closed state.

RESULTS AND DISCUSSION

ATP Binding Process

After equilibration of the available MurD crystal structures TMD simulations were initiated utilizing pairs of boundary structures. In each time step the RMSD between two structures was reduced and the trajectories reached the target conformation in ~1 ns. In both open structures, 1E0D and 1EEH the starting positions of ATP and UMA were from 20 Å to 30 Å away from the enzyme. The calculated TMD trajectories enabled study of the binding order and observation of interactions with the enzyme for both ligands. The data for substrate binding order are not known for MurD, nevertheless it is safe to assume that they do not differ significantly from the binding order experimentally determined for MurC and MurF because of the experimentally elucidated functional and structural resemblance of this enzyme family.

Analysis of both TMD trajectories indicated that overall in the first part of the trajectory ATP and UMA move towards their binding sites, followed by the closing period where the majority of C-terminal domain rotation occurs forming the active conformation of MurD. The conformational transition of the C-terminal domain does not occur before ATP binding; however small conformational changes leading to MurD closure are already noticeable during UMA binding. This observation fits well with the experimental suggestions that ATP is required to induce the domain closure.

In 1EEH-2UAG and 1E0D-2UAG trajectories, ATP interacts fully with its active site before UMA starts to move towards the enzyme, as is evident from the comparison of the ligands' temporal distance graphs in Figures 3(A) and 4(A) outlined for the 1EEH-2UAG trajectory. When approaching the active site, ATP also carries

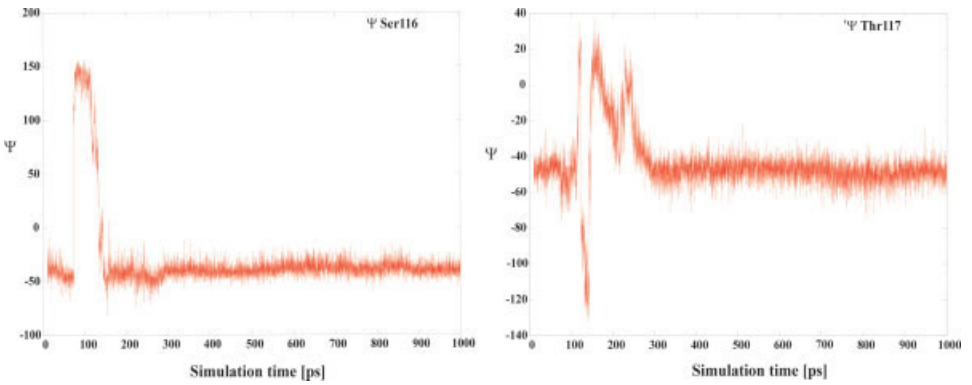

Fig. 2. Large conformational displacement of ψ dihedral torsion angles of Ser116 and Thr117, components of the α6 helix in the ATP binding process (1EEH-2UAG trajectory). [Color figure can be viewed in the online issue, which is available at www.interscience.wiley.com.]

one magnesium ion coordinated between the β-and γ-phosphate groups. When ATP enters the binding site it first interacts with Gly114, Ser116, and Thr117 which play an important role in proper positioning of the γ-phosphate group of ATP towards Lys115. Strong coordination between the β- and γ-phosphate of ATP and Lys115 [Fig. 3(B1)] represents the first important interaction in the ATP binding process. Lysine positioned between the β- and γ- phosphates of ATP was also observed in MurC AMP-PNP analogues[39] and is present in several NTP-binding proteins with bounded nucleotide or its analogue as well[40,41] where it plays a crucial role in binding and subsequent enzyme catalysis.

One interesting conformational change that was observed in the 1EEH-2UAG trajectory was the partial unfolding of the α6 helix on the N-terminal domain when ATP approaches the active site. The sequence of the three amino acid residues Thr117, Ser116, and Lys115 of this helix unfolds as Ser116 starts to interact with the magnesium ion coordinated between β- and γ-phosphate. The α6 helix was subsequently reformed in the original conformation as can be effectively monitored by the drastic change in the ψ torsion angles of Ser116 and Thr117. This "torsional swing" depicted in Figure 2 for the involved residues Ser116 and Thr117 enabled the interaction of β-and γ-phosphate of ATP with Lys115.

The next step in the ATP recognition process differs slightly between the trajectories. In the 1EEH-2UAG trajectory, the adenine moiety of ATP interacts with the amide side chain of residue Asn271, thus anchoring ATP firmly on the molecular surface of the MurD central domain. Subsequent interaction with the guanidine side chain of Arg302, which is accompanied by a large displacement of this residue side chain, is concurrent with the initiation of C-terminal domain closure as discussed further in Conformational transition of the C-terminal domain of *E.coli* Mur D Section. This result corroborates with the experimental observation by Dideberg and coworkers who observed a large side chain movement in Arg302.[6]

On the other hand, in 1E0H-2UAG simulation an almost concurrent onset of interactions with Arg302 and Asn271 moves ATP into a binding position similar to the one observed in the crystal structure. This can be attributed to the fact that Arg302 in 1E0D open structure is not significantly displaced from its position observed in the closed structure. Interestingly, in 1E0D-2UAG simulation, in the course of ATP binding the nitrogen of the guanidine moiety of Arg302 first interacts with ATP and further docking of ATP into the active site accommodates the Arg302 side chain into an X-ray observed conformation. Again, Arg302 motion is simultaneous with the C-terminal domain closure and proper positioning of this residue could be interpreted as one of the structural triggers that initiate the C-domain closure in both structures. Despite the difference in C-terminal domain position in the experimental crystal structure the largest side chain movement was also observed for this residue.

The principal rotation of the C-terminal domain of MurD that commences slowly after ATP fixation finally brings the OD1 oxygen of Asp317 from a distance of about 20 Å to a hydrogen bond distance of ATP O3* oxygen [Fig. 3(B2)] observed in the crystal structure. The displacement of the carboxylic group of Asn317 in the closed state is minimal.

UMA Binding Process

After the ATP molecule is firmly positioned in its binding site that is located predominately on the MurD central domain UMA as the UDP precursor commences its approach to its binding site. Figure 4(A) shows temporal graphs depicting the distances of selected pairs of atoms on UMA and MurD that were found in the hydrogen bond distance in the closed structure.

The magnesium ion that acts as a bridge between the anionic moieties of UMA and ATP in the closed structure was found to play a crucial role in UMA binding. The first interaction of UMA with the MurD molecular surface, observed in both TMD trajectories, is the magnesium-assisted coordination of UMA carboxylate on one side and residues His183 and carbamylated Lys198 on the other, both of which form the magnesium binding site previously proposed [Fig. 4(B1)].[6] These residues are located on the loop between β9 and α9 helix of the MurD

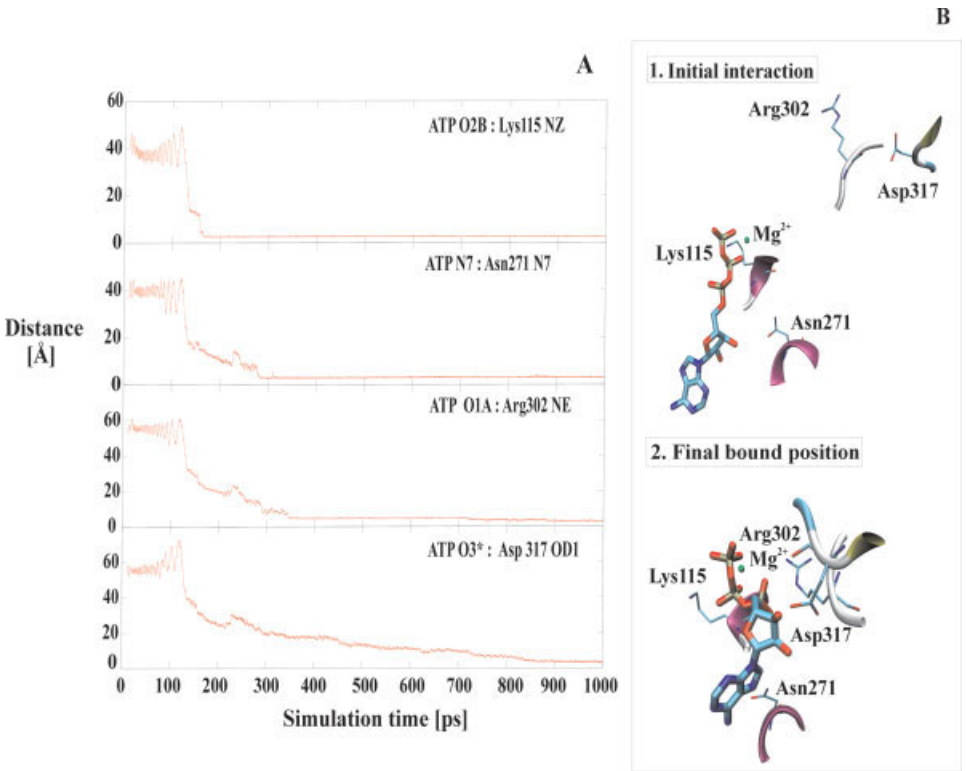

Fig. 3. ATP binding process outlined for the 1EEH-2UAG trajectory. (**A**) Distances between elements of ATP and the corresponding selected residues located in the MurD ATP active site. (**B**) Snapshots from the TMD trajectory depicting the atomistic details of the initial ATP contact with its active site and final bound ATP conformation. [Color figure can be viewed in the online issue, which is available at www.interscience.wiley.com.]

central domain and thus seem to play together with magnesium ion an indirect role in UMA recognition. In the 1EEH open structure, the loop between the β9 and α9 helix (residues 176–190) was fully resolved in the electron density map. Analyses of the 1E0D-2UAG trajectory, in which residues in the loops between 183 and 188 had to be modeled because of their absence in the 1E0D crystal structure, has shown that this interaction is observed in both TMD trajectories and provides additional evidence of the His183 role in indirect UMA binding as indicated in previous structural studies.[6] Further experimental evidence of the importance of His183 in successful UMA binding was added by constructing mutant MurD His183Ala where UMA binding affinity was substantionally reduced.[10]

Following initial interaction with UMA a large conformational displacement is observed in the loop between the β9 and α9 helix. As a result His183 and modified Lys198 slowly drag the carboxylic part of the molecule towards the active site where the alanine sub-moiety of UMA interacts with Asn138 that accommodates the UMA terminal part to the final conformation. Almost concurrently with this process, UMA forms hydrogen bonds with several residues elucidated from previous structural studies as responsible for UMA binding. The residues Gly73, Gln162, Thr16, and Leu15 attach UMA firmly into the active site [Fig. 4(B2)]. The uracile moiety is the last to enter the UMA active site forming interactions with Thr36 to complete the UMA binding. The suggested role of carbamylated Lys198 in the UMA binding was confirmed in both TMD trajectories thus providing additional agreement with biochemical experiments that elucidated its functional importance[24] in the formation of magnesium binding site formation.

Analyses of the 1E0D-2UAG trajectory has shown that when UMA is dragged into its active site, the protein loop located on the central domain between α7 and β7 has to readjust its backbone conformation in order to avoid a steric clash with the substrate. As UMA binds to its active site, this loop folds over its muramoyl moiety to adapt into the conformation observed in the closed MurD. Systematic analysis of loops backbone torsional angles identified the ψ dihedral angle of Gly140 as being vital in enabling the transition, by moving from values around −120° to about 10° as presented on Figure 5. Again, this observation fits well with the conclusion drawn from the comparison of the open and closed structures of MurD, where this structural difference was first identified.[7]

Conformational Transition of the C-Terminal Domain of *E. coli* MurD

The overall graphical representation of the C-terminal domain rotation outlined for the 1EEH-2UAG trajectory

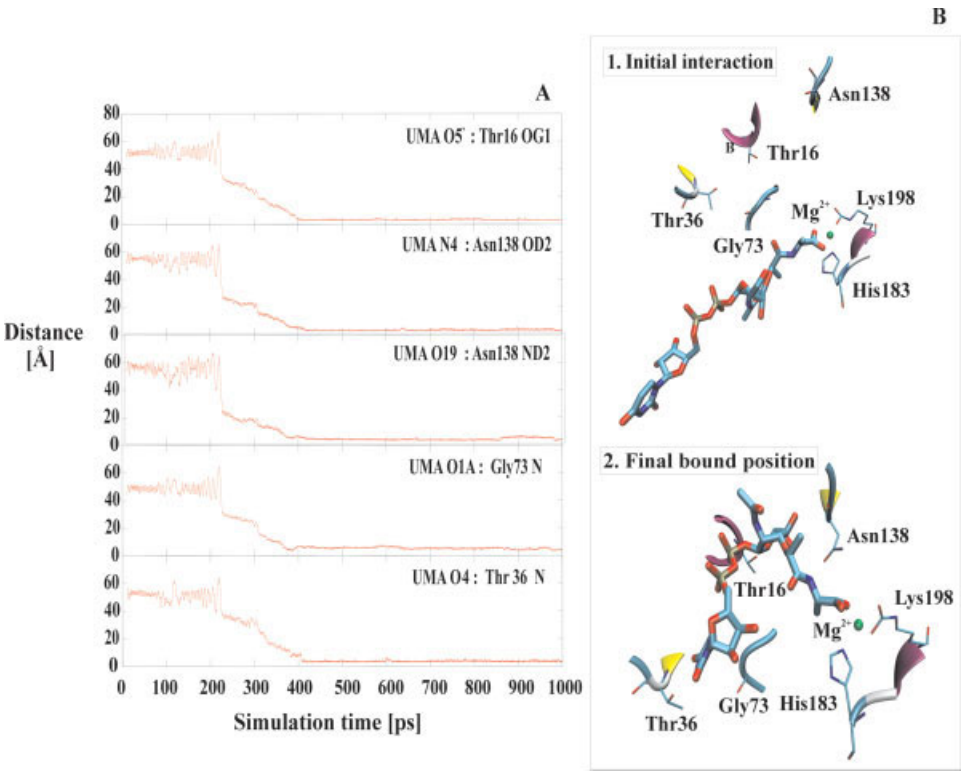

Fig. 4. Substrate UMA binding process outlined the 1EEH-2UAG trajectory. (**A**) Distances between elements of UMA and the corresponding residues. Time is set to describe the trajectory from open to closed conformation. (**B**) Snapshots from TMD trajectory depicting the initial UMA contact with its active site and its final binding position. [Color figure can be viewed in the online issue, which is available at www.interscience.wiley.com.]

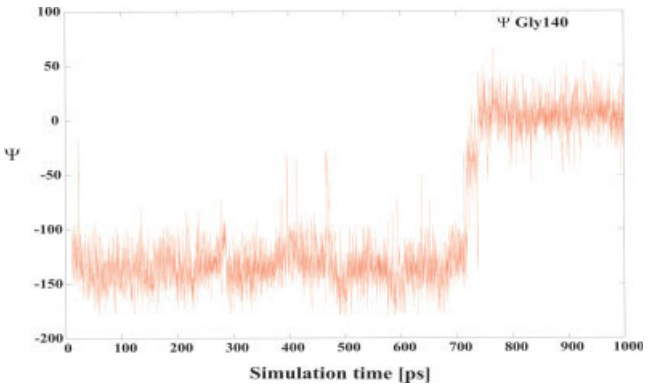

Fig. 5. Ψ backbone torsion angle of Gly140 located in the loop between α7 and β7 involved in the conformational changes observed between UMA binding. [Color figure can be viewed in the online issue, which is available at www.interscience.wiley.com.]

can be observed in Figure 6(A), where the C-terminal domain moves into the plane of the N-terminal domain and central domain of MurD. Additionally, in Figure 6(B), only the connecting part of the C-terminal domain and central domain are depicted. This should facilitate a comparison with 1E0D-2UAG trajectory, which is depicted identically in Figure 7(B) and will be discussed below.

Based on the results of structural studies on MurD it was proposed that the rigid body rotation of the C-terminal domain is required to bring the structure from open to its closed form.[7] Visual analysis of secondary structural elements (α-helices, β sheets and turns) and the C-terminal domain overall tertiary structure in 1EEH-2UAG and 1E0D-2UAG trajectories revealed only smaller deviations within this domain during the TMD transition. To quantify this observation RMSD values were calculated between the C-terminal domain of the snapshots obtained for every 100 ps of the TMD simulation and superimposed C-terminal domain of the relaxed 2UAG structure. The flexible loop connecting the C-terminal domain with central domain was excluded form RMSD calculations so backbone atoms of the residues 305–437 only were included in the comparison. As presented in Table 1 for the 1EEH-2UAG trajectory a slight increase of backbone RMSD during the first stages of the transition was noticed however RMSD value still deviate only at about 1–1.5 Å higher displacement during the transition compared with the RMSD of the relaxed boundary structures.

To elucidate the source of the observed RMSD increase a careful analysis of the domain secondary structures revealed two changes in the domain elements. The partial defolding of MurD α12 helix and smaller displacement of α13 helix were found to be the main reasons for the observed RMSD increase. Residues from Val323 to Thr326 of α12 are no longer in α-helix conformation

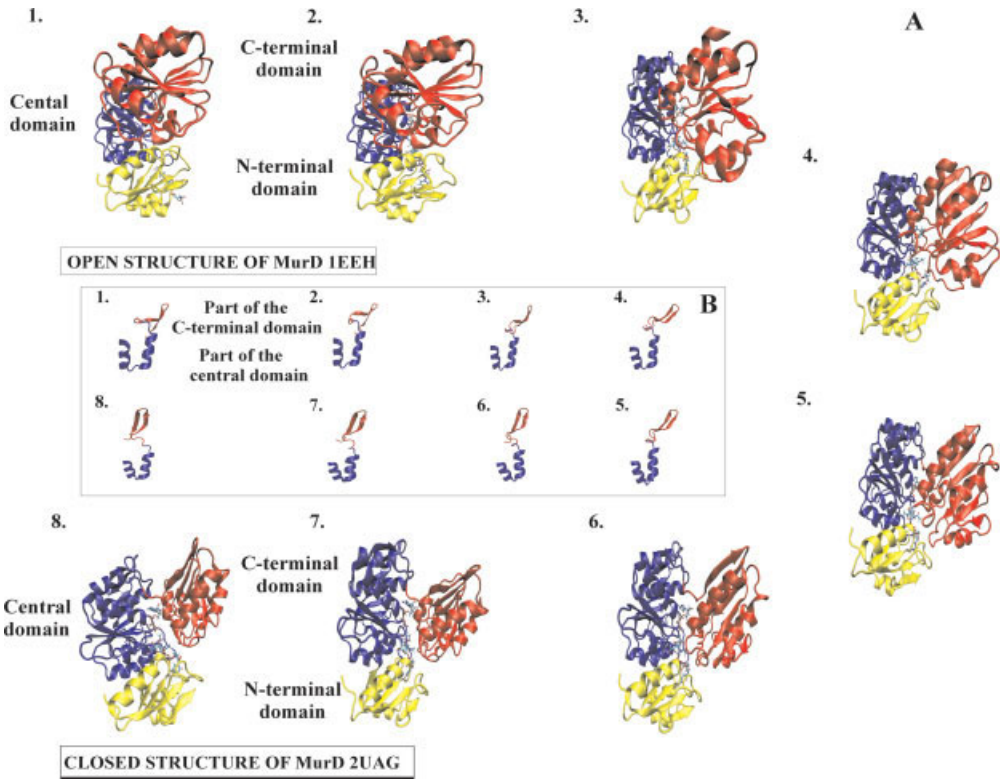

Fig. 6. Snapshots from 1EEH-2UAG simulation denoting the rigid body rotation of the C-terminal domain. (**A**) Rigid body rotation of C-termin al domain of MurD. The C-terminal domain rotates out of the original plane and rests on the top of N-and central domain (**B**) Rotation displayed for small fragments of C-terminal and central domain to allow better comparison with 1EEH-2UAG trajectory. [Color figure can be viewed in the online issue, which is available at www.interscience.wiley.com.]

after about 60 ps of the simulation; however no larger movement of C-terminal domain is observed before the ATP binds to the enzyme. As Arg302 moves to interact with ATP a major movement of α12 helix is observed as it slides over the surface of α7 helix and loop connecting this helix to β7 to come to the plane of central and N-terminal domain The defolded part of α12 helix is fully reformed at $\sim$700 ps when this domain motion is complete and when the final part of the C-terminal domain closure occurs. RMSD values of the 1EEH-2UAG trajectory (Table 1) deviate around the RMSD value observed between the boundary structures at about 1 Å. As a large majority of the elements of the C terminal domain do not change during the transition the rotational motion can still be treated as a rigid body rotation.

To determine which torsion angles are involved in the C-terminal domain transition and to gain deeper insight into the rotation process a systematic search of the ψ and ϕ dihedral torsion angles of the loop connecting α11 of the central domain and β15 of the C-terminal domain was conducted for both calculated trajectories. A total of 20 backbone dihedral torsion angles were analyzed in each case; involving residues Thr295 to Glu304.

In the 1EEH-2UAG trajectory several residues are involved in the rotation of this domain. The residue that exhibited the largest torsion displacement during C-terminal domain rotational motion is located in the middle of the loop. The ϕ torsion angle of conformationally constrained amino acid Pro300 acts as an axis around which the C-terminal domain is brought to the closed conformation. The ψ Pro300 angle moves from values of around -50° in a rather monotonous fashion to final values of around 150°. In Figure 8 it is evident that the majority of conformational transition starts at around 300 ps. A large displacement in the ψ backbone angle of Arg302 can be seen at about 250 ps from 160° to about 100°. The dihedral value then fluctuates and slowly, at about 400 ps, reaches the values observed in the closed structure. Comparison of torsion graphs for ψ of Arg302 and ψ for Pro300 suggests that Pro300 conformational change follows the accommodation of Arg302 that occurs due to ATP binding. These results fit well with the suggested role of ATP as being required to induce the domain closure that was briefly discussed in ATP Binding Process Section.[7] This part of the rotational motion lifts the C-terminal domain from its open position into a position above the rest of the enzyme [Fig. 6(A1–4)]. In the final stages, the domain rotates towards the plane where the N-terminal and central domain are located [Fig. 6(A5–8)]. Residues Leu299 and Gly298 play an important role in this part of the transition. At about 700 ps,

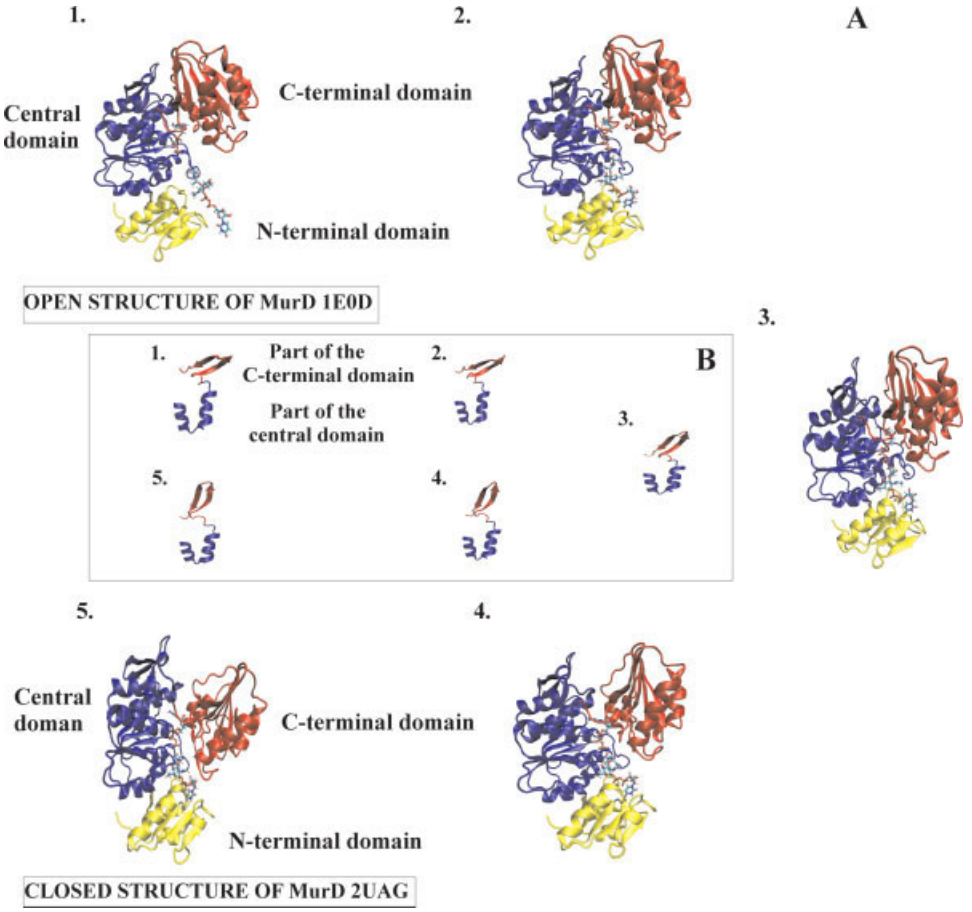

Fig. 7. Snapshots from 1E0D-2UAG simulation illustrating the rigid body rotation of the C-terminal domain. (**A**) The final position of the C-terminal domain remains in the same plane as the central and N-terminal domain. (**B**) Rotation displayed for small fragments of the C-terminal and central domain and the connecting loop to allow better comparison with them 1E0D-2UAG trajectory. [Color figure can be viewed in the online issue, which is available at www.interscience.wiley.com.]

TABLE I. Comparison of the C-terminal Domain Backbone Atoms Structure with C-Terminal Domain of Closed (2UAG) Structure After Relaxation

Simulation time (ps)	RMSD 1E0D-2UAG trajectory (Å)	Relative RMSD (Å)	RMSD 1EEH-2UAG trajectory (Å)	Relative RMSD (Å)
0	1.01	—	1.37	—
100	0.95	−0.06	2.17	0.80
200	1.05	0.04	2.05	0.68
300	0.87	−0.14	2.95	1.58
400	0.84	−0.17	2.99	1.62
500	0.90	−0.11	2.97	1.60
600	0.99	−0.02	2.44	1.07
700	1.03	0.02	1.72	0.35
800	1.21	0.20	1.21	−0.16
900	0.92	−0.11	0.86	−0.77
1000	0.00	0.00	0.00	0.00

Time is set in the reverse direction describing open to closed transition. Calculated RMSD values of the C-terminal domain backbone atoms between relaxed boundary structure 2UAG and snapshots obtained from 1E0D-2UAG and 1EEH-2UAG TMD simulations, respectively (cols 2,4). Relative RMSD differences between the RMSD of the relaxed boundary structure 2UAG and the snapshot RMSD (cols 3,5).

as seen on Figure 8, for the 1EEH-2UAG trajectory the value of ϕ dihedral angle value of Leu299 rapidly changes from 50° to 100° and this motion reorients the loop so that this residue together with a flexible Gly298 induce the final rotation of C-terminal domain to its target conformation.

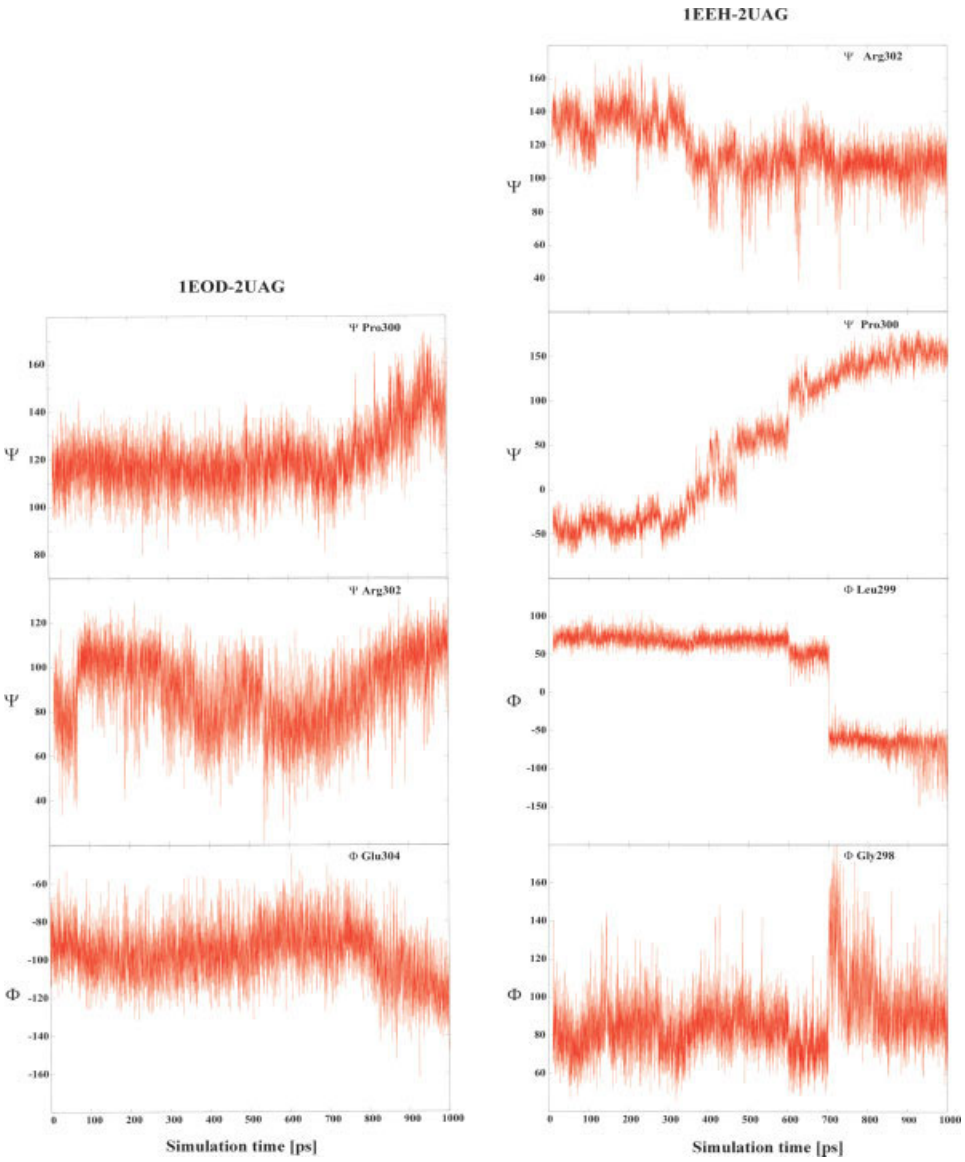

Fig. 8. Backbone torsion angles of the selected residues of the loop connecting α11 of the central domain and β15 of the C-terminal domain during TMD simulations. [Color figure can be viewed in the online issue, which is available at www.interscience.wiley.com.]

The second simulation yielding the 1E0D-2UAG trajectory revealed no significant conformational changes of the C-terminal domain during TMD simulation. Moreover, the backbone RMSD values for the C-terminal domain calculated for the snapshots from the TMD simulation and relaxed 2UAG crystal structure were comparable with RMSD for C-terminal domain between experimental 1E0D and 2UAG structures which lays around 0.72 Å for the selected residues 305 to 437 (Table 1). A careful visual analysis of the secondary structure elements revealed no significant deviations as well.

The C-terminal domain rotation in 1E0D-2UAG trajectory is outlined in Figure 7(A). Additionally, in Figure 7(B) the connecting parts of the C-terminal and central domain are depicted. This should enable a better comparison with previously discussed 1E0D-2UAG trajectory.

Twenty backbone dihedral torsion angles of loop 295–304, were analyzed to see which residues play the most significant role in the conformational transition and the results obtained show the residues that exhibited the largest torsion displacement during domain rotational motion are located in the middle of the loop. Again, the ϕ torsion angle of the conformationally constrained amino acid Pro300 was identified as an axis around which the C-terminal domain is brought slowly to the closed conformation. The torsion angle changes from a value 120° to about 145°.

In the course of domain closure one more residue on the connecting loop was identified as being important.

At the end of the loop, near the beginning of the C-terminal domain the ϕ torsion angle of Glu304 moves from -100° to -140° and assists in the proper closing motion of the C-terminal domain [Fig. 8]. However, a synchronized motion of the entire loop is required to bring this domain to the closed conformation.

CONCLUSIONS AND IMPLICATIONS

The present investigation is an attempt to gain insight into the binding process of UMA and ATP and to describe conformational transition of the C-terminal domain in MurD structure at the atomistic level, exploiting a well-established TMD method. As TMD procedure finds a successive configuration, which can is obtained from the previous one with minimum energy expenditure, the performed reverse course of simulations (closed to open state) permitted us a better starting configuration for the simulation than it would be the open structure with arbitrary positions of ligands. It is noteworthy to state that in both simulations the ligand binding order was in accordance with the biochemical experimental data. The ATP molecule binds in both trajectories first to MurD with the substrate UMA following in second. The roles of carbamylated Lys198 and His183 as the first UMA interacting residues are observed in both simulations and are in agreement with their proposed function as residues directing UMA into its binding site. Magnesium ions play an important role in the binding of both ligands. However, despite the fact that TMD results in two simulations we performed correspond well with the experimental findings a caveat must clearly be stated that drawing conclusions on the binding order and the ligands binding process involving large protein displacement from equilibrium simulations of unbinding would need more elaborate study.

When UMA and ATP are already well positioned into their sites rotation of the C- terminal domain brings the enzyme to its active conformation. Apart from the temporally limited distortion of the α12 helix and a small displacement of α13 helix that were detected in the 1EEH-2UAG trajectory the secondary structure elements together with the overall tertiary structure of the C-terminal domain do not change significantly thus indicating rigid body rotation as the overall rotation motion that was quantified by a RMSD analysis of the snapshots form the TMD simulation. The observed change in the Arg302 side chain position and subsequent backbone displacement as this residue interacts with ATP temporally corresponded with the induction of domain closure in both trajectories despite the difference in the position of the moving domain. This provides additional support to previous suggestions that ATP is required to induce the domain closure.

Analysis of backbone torsion angles of residues in the loop connecting the central and C-terminal domain indicated the residue Pro300 as the main axis of the domain rotation. However, the rotational motion is not isolated to this residue as concurrent cooperation of several residues is required for successful closure. In the 1EEH-2UAG trajectory our analysis revealed that residues Leu299 and Gly298 also contribute to the proper rotation motion.

There are analogous protein movements described in the literature in which the importance of resolving the details of the binding site in order to perform meaningful structure-based drug design was stressed. For example, the problem of the meagre array of hits even for focused chemical libraries in the case of Hepatitis C virus (HCV) helicase has been well documented.[42] It appears that the principal reason for this has been the variable separation of Domains 1 and 2 in HCV helicase, which complicate the topology of the potential target-binding site. New information regarding the possible conformational pathway of the MurD ligase along with the elucidation of detailed interactions required for UMA and ATP binding will hopefully enable an improved design of MurD inhibitors. Due to close functional resemblance of the ligase family TMD results also lead towards a deeper understanding of the common mechanism of these bacterial enzymes.

ACKNOWLEDGMENTS

The authors wish to thank Dr. E. Hutton for critical reading of the manuscript and Urban Borštnik for helpful technical assistance.

REFERENCES

1. Brown ED, Wright GD. New targets and screening approaches in antimicrobial drug discovery. Chem Rev 2005;309:759–774.
2. Silver LL. Does the cell wall of bacteria remain a viable source of targets for novel antibiotics? Biochem Pharmacol 2006;71: 996–1005.
3. van Heijenoort J. Recent advances in the formation of the bacterial peptidoglycan monomer unit. Nat Prod Rep 2001;18:503–519.
4. Zoeiby AE, Sanschagrin F, Levesque RC. Structure and function of the Mur enzymes: development of novel Inhibitors. Mol Microbiol 2003;47:1–12.
5. Bertrand JA, Auger G, Fanchon E, Martin L, Blanot D, van Heijenoort J, Dideberg O. Crystal structure of UDP-*N*-acetylmuramoyl-L-alanine:D-glutamate ligase from *Escherichia coli*. EMBO J 1997;16:3416–3425.
6. Bertrand JA, Auger G, Martin L, Fanchon E, Blanot D, Le Beller D, van Heijenoort J, Dideberg O. Determination of the MurD mechanism through crystallographic analysis of enzyme complexes. J Mol Biol 1999;289:579–590.
7. Bertrand JA, Fanchon E, Martin L, Chantalat L, Auger G, Blanot D, van Heijenoort J, Dideberg O. "Open" structures of MurD: domain movements and structural similarities with folylpolyglutamate synthetase. J Mol Biol 2000;301:1257–1266.
8. Anderson MS, Eveland SS, Onishi HR, Pompliano DL. Kinetic mechanism of the *Escherichia coli* UDPMurNAc-tripeptide D-alanyl-D-alanine-adding enzyme: use of a glutathione *S*-transferase fusion. Biochemistry 1996;35:16264–16269.
9. Emanuele JJ Jr, Jin H, Yanchunas J Jr, Villafranca JJ. Evaluation of the kinetic mechanism of *Escherichia coli* uridine diphosphate-*N*-acetylmuramate:L-alanine ligase. Biochemistry 1997;36: 7264–7271.
10. Bouhss A, Dementin S, Parquet C, Mengin-Lecreulx D, Bertrand JA, Le Beller D, Dideberg O, van Heijenoort J, Blanot D. Role of the ortholog and paralog amino acid invariants in the active site of the UDP-MurNAc-L-alanine:D-glutamate ligase (MurD). Biochemistry 1999;38:12240–12247.

11. Ikeda M, Wachi M, Jung HK, Ishino F, Matsunashi M. Homology among MurC, MurD, MurE and MurF proteins in *Escherichia coli* and that between *E. coli* MurG and a possible MurG protein in *Bacillus subtilis*. J Gen Appl Microbiol 1990;36:179–187.
12. Yan Y, Munshi S, Leiting B, Anderson MS, Chrzas J, Chen Z. Crystal structure of *Escherichia coli* UDPMurNAc-tripeptide-D-alanyl-D-alanine-adding enzyme (MurF) at 2.3A resolution. J Mol Biol 2000;304:435–445.
13. Longenecker KL, Stamper GF, Hajduk PJ, Fry EH, Jakob CG, Harlan JE, Edalji R, Bartley DM, Walter KA, Solomon LR, Holzman TF, Gu YG, Lerner CG, Beutel BA, Stoll VS. Structure of MurF from *Streptococcus pneumoniae* co-crystallized with a small molecule inhibitor exhibits interdomain closure. Protein Sci 2005;14:3039–3047.
14. Karplus M, McCammon JA. Molecular dynamics simulations of biomolecules. Nat Struct Biol 2002;9:646–652.
15. Karplus M, Kuriyan J. Molecular dynamics and protein function. Proc Natl Acad Sci USA 2005;102:6679–6685.
16. Adcock SA, McCammon JA. Molecular dynamics: survey of methods for simulating the activity of proteins. Chem Rev 2006; 106:1589–1615.
17. Schlitter J, Engels M, Krüger P. Targeted molecular dynamics: a new approach for searching pathways of conformational transitions. Mol Graph 1994;12:84–89.
18. Schlitter J, Engels M, Kruger P, Jacoby EU, Wollmer A. Targeted molecular dynamics simulation of conformational change: application to the TR transition in insulin. Mol Simul 1993;10:291–308.
19. Krüger P, Verheyden S, Declerck PJ, Engelborghs Y. Extending the capabilities of targeted molecular dynamics: simulation of a large conformational transition in plasminogen activator inhibitor 1. Protein Sci 2001;10:798–808.
20. Mendieta J, Gago F, Ramírez G. Binding of 5′-GMP to the GluR2 AMPA receptor: insight from targeted molecular dynamics simulations. Biochemistry 2005;44:14470–14476.
21. Lee HS, Robinson RC, Joo CH, Lee H, Kim YK, Choe H. Targeted molecular dynamics simulation studies of calcium binding and conformational change in the C-terminal half of gelsolin. Biochem Biophys Res Commun 2006;342:702–709.
22. Borištnik U, Hodošček M, Janežič D. Improving the performance of molecular dynamics simulations on parallel clusters. J Chem Inf Comput Sci 2004;44:359–364.
23. Brooks BR, Bruccoleri RE, Olafson BD, States DJ, Swaminathen S, Karplus M. CHARMM: a program for macromolecular energy, minimization, and dynamics calculations. J Comput Chem 1983; 4:187–217.
24. Dementin S, Bouhss A, Auger G, Parquet C, Mengin-Lecreulx D, Dideberg O, van Heijenoort J, Blanot D. Evidence of a functional requirement for a carbamoylated lysine residue in MurD, MurE and MurF synthetases as established by chemical rescue experiments. Eur J Biochem 2001;268:5800–5008.
25. Gordon E, Flouret B, Chantalat L, van Heijenoort J, Mengin-Lecreulx D, Dideberg O. Crystal structure of UDP-*N*-acetylmuramoyl-L-alanyl-D-glutamate: *meso*-diaminopimelate ligase from *Escherichia coli*. J Biol Chem 2001;276:10999–11006.
26. MacKerell AD Jr, Bashford D, Bellott M, Dunbrack RL Jr, Evanseck JD, Field MJ, Fischer S, Gao J, Guo H, Ha S, Joseph-McCarthy D, Kuchnir L, Kuczera K, Lau FTK, Mattos C, Michnick S, Ngo T, Nguyen DT, Prodhom B, Reiher WE III, Roux B, Schlenkrich M, Smith JC, Stote R, Straub J, Watanabe M, Wiorkiewicz-Kuczera J, Yin D, Karplus M. All-atom empirical potential for molecular modeling and dynamics Studies of proteins. J Phys Chem B 1998;102:3586–3616.
27. MacKerell AD Jr, Feig M, Brooks CL III. Extending the treatment of backbone energetics in protein force fields: limitations of gas-phase quantum mechanics in reproducing protein conformational distributions in molecular dynamics simulations. J Comput Chem 2004;25:1400–1415.
28. Foloppe N, MacKerell AD Jr. All-atom empirical force field for nucleic acids. I. Parameter optimization based on small molecule and condensed phase macromolecular target data. J Comput Chem 2004;25:86–104.
29. MacKerell AD Jr, Banavali NK. All-atom empirical force field for nucleic acids. II. Application to molecular dynamics simulations of DNA and RNA in solution. J Comput Chem 2004;25: 105–120.
30. Jorgensen WL, Chandrasekhar J, Madura JD, Impey RW, Klein ML. Comparison of simple potential functions for simulating liquid water. J Chem Phys 1983;79:926–935.
31. Essman U, Perera L, Berkowitz ML, Darden T, Lee H, Pedersen A. A smooth particle mesh Ewald method. J Chem Phys 1995; 103:8577–8593.
32. Im W, Lee MS, Brooks CL III. Generalized born model with a simple smoothing function. J Comput Chem 2003;24:1691–1702.
33. Nina M, Beglov D, Roux B. Atomic Born radii for continuum electrostatic calculations based on molecular dynamics free energy simulations. J Phys Chem B 1997;101:5239–5248.
34. Humphrey W, Dalke A, Schulten K. VMD: visual molecular dynamics. J Mol Graph 1996;14:33–38.
35. Frishman D, Argos P. Knowledge-based protein secondary structure assignment. Proteins: Struct Funct Genet 1995;23:566–579.
36. http://www.gnuplot.info.
37. Torrie G, Valleau J. Nonphysical sampling distributions in Monte Carlo free-energy estimation: umbrella sampling. J Comput Phys 1997:23;187–199.
38. Allen M, Tildesley D. Computer simulation of liquids. New York: Oxford University Press; 1987.
39. Mol CD, Brooun A, Dougan DR, Hilgers MT, Tari LW, Wijnands RA, Knuth MW, McRee DE, Swanson J. Crystal structures of active fully assembled substrate- and product-bound complexes of UDP-*N*-acetylmuramic acid:L-alanine ligase (MurC) from *Haemophilus influenzae*. J Bacteriol 2003;185: 4152–4162.
40. Kjeldgaard M, Nissen P, Thirup S, Nyborg J. The crystal structure of elongation factor EF-Tu from *Thermus aquaticus* in the GTP conformation. Structure 1993;1:35–50.
41. Pai EF, Krengel U, Petsko GA, Goody RS, Kabsch W, Wittinghofer A. Refined crystal structure of the triphosphate conformation of H-ras p21 at 1.35 A resolution: implications for the mechanism of GTP hydrolysis. EMBO J 1990;9:2351–2359.
42. Kwong AD, Rao BG, Jeang KT. Viral and cellular RNA helicases as antiviral targets. Nat Rev Drug Discov 2005;4:845–853.